Quadrupolelike electrostatic guiding for cold polar molecules

Yong Xia, Yaling Yin, Haibo Chen, Lianzhong Deng, and Jianping Yin[a)]
State Key Laboratory of Precision Spectroscopy, and Department of Physics, East China Normal University, Shanghai 200062, People's Republic of China

(Received 26 July 2007; accepted 31 December 2007; published online 3 March 2008)

We demonstrate electrostatic guiding of cold heavy water (D_2O) molecules over a distance of 44.5 cm by using a quadrupolelike electrostatic field, which is generated by the combination of two parallel charged poles and two grounded metal plates. We measure the transverse spatial distribution of the guided D_2O molecular beam and study the dependence of the relative guiding efficiency and the transverse temperature of the guided molecular beam on the guiding voltage. Our study shows that the maximum guiding efficiency of ~50% can be obtained, and our experimental results are in good agreement with ones of theoretical calculation and Monte Carlo simulations, and this guiding scheme has some potential applications in molecule optics, such as molecular-beam splitter, integrated molecular optics, etc. © *2008 American Institute of Physics*. [DOI: 10.1063/1.2837462]

I. INTRODUCTION

It is well known that cold molecules offer some new opportunities for molecular spectroscopy and precision measurements,[1] molecular collisions and cold chemistry,[2,3] and so on. Especially, new applications of cold polar molecules in quantum computing and its information processing[4,5] have attracted increasing interests in recent years. Using the interaction of the molecular electric dipole moment with an inhomogeneous electrostatic field, polar molecules can be decelerated,[6,7] trapped,[8] and manipulated.[9–16] When the average orientation of the molecular electric dipole moments is parallel or antiparallel to the local electric field, the polar molecules in the high-field-seeking (HFS) states will be attracted to the maximum of the electrostatic field, or the molecules in the low-field-seeking (LFS) states will be repulsed to the minimum of the electric field. In 2000, Loesch and Scheel demonstrated a Keppler electrostatic guiding of cold polar molecules (NaCl, NaBr, NaI) in the HFS states and obtained the maximum guiding efficiency of ~0.12%.[11] Recently, Rempe and co-workers realized the quadrupole electrostatic guiding of cold polar molecules (such as H_2CO, ND_3 and D_2O) in the LFS states or in the HFS ones from an effusive molecular beam by using a standard quadrupole electrostatic field, which was generated by four charged poles,[12–14] but its guiding efficiency did not be reported. This scheme cannot only be used to guide cold polar molecules in the LFS or HFS states, but also to generate cold molecular beam by the low-pass energy filter based on the bend molecular guiding. More recently, two novel and simpler schemes to guide cold polar molecules using a hollow electrostatic field generated by the combination of two parallel charged poles and a ground metal plate or by the combination of a single charged pole and two parallel ground metal plates were proposed.[15,16] In this paper, we demonstrate a new scheme to guide cold polar molecules by using a quadrupolelike electrostatic field, which is generated by the combination of two parallel charged poles and two parallel ground metal plates, and measure the transverse spatial distribution of the guided supersonic D_2O molecular beam, and study the dependence of the relative guiding efficiency and the transverse temperature of the guided molecular beam on the guiding voltage. Also, we study the dynamic guiding process of cold polar molecules by using the theory model and Monte Carlo simulations, and briefly discuss some potential applications of our guiding scheme in molecule optics.

II. EXPERIMENTAL SETUP

Figure 1 shows our experimental setup, which consists of a compact supersonic molecular beam system with two differentially pumped vacuum chambers and a molecular guiding system. The locations of each element and their sizes in our guiding system with respect to the nozzle of the solenoid valve are summarized in Fig. 1(b). The experiment has been performed with the heavy water (D_2O) seeded in the argon carrier gas. A pulsed supersonic beam of D_2O is formed by adiabatically expanding a gaseous mixture, 1.2% heavy water vapor evaporated at room temperature with an argon carrier gas through a solenoid valve (General Valve, Series 9, ∅0.5 mm) into vacuum, and its stagnation pressure is 2.0 atm. The operating pressure in the source chamber and the guiding one are typically $\sim 2.0\times10^{-3}$ and $\sim 3.0\times10^{-6}$ Pa, respectively. The molecular beam passes through a skimmer with a diameter of 1.0 mm into the guiding chamber, and then flies into a 50 mm long hexapole electrostatic field, which play the states selecting and focusing function as a positive lens for polar molecules in the LFS states, and here the hexapole (HP) is made of six stainless steel rods with a 3.0 mm diameter placed equidistantly on a circles with a 4.5 mm radius and ±8.0 kV. The state-selected and focused molecules will be efficiently coupled into and guided in the hollow quadrupolelike electrostatic field generated by the combination of a pair of parallel charged stain-

[a)]Author to whom correspondence should be addressed. Electronic mail: jpyin@phy.ecnu.edu.cn.

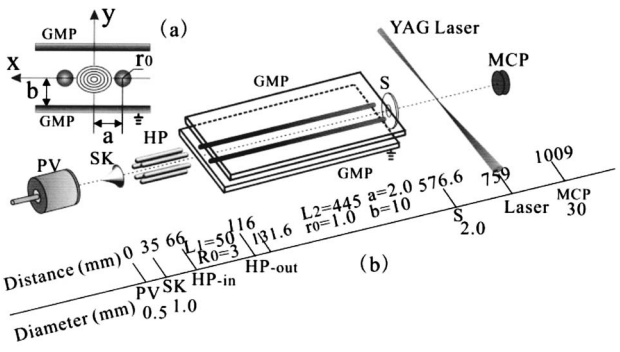

FIG. 1. (a) Cross-sectional view of a pair of parallel charged stainless steel rods and two grounded metal plates; (b) sketch map of the experimental apparatus and the locations of each element in front of the nozzle and their sizes. PV, SK, HP, GMP, and S stand for pulse valve, skimmer, hexapole, grounded metal plate, and sampling hole, respectively.

less steel rods (electrodes) and two grounded metal plates, and then the output molecular beam from a sampling small hole with a radius of 1.0 mm is ionized by the frequency-quadrupled output of a Nd:YAG (yttrium aluminum garnet) laser (Continuum Surelite I-10, 266 nm, 5 ns) with a single-pulse energy of 10.5 mJ. The D_2O ions were collected and accelerated into time-of-flight mass spectrometer with Wiley-McLaren type, and finally detected by dual microchannel plates (MCP) in Chevron configuration (operated at a gain of 10^6). The signals from the MCP output were collected and averaged on an oscilloscope (HP 54616C, 500 MHz), whose output was transferred to the personal computer for signal storage and processing.

For simplicity, the (x,y,z) coordinates are set as shown in Fig. 1(a), and the guiding direction of cold molecular beam is parallel to the z-axis. The cross-sectional diagram of the guide apparatus is shown in Fig. 1(a). In our guiding experiment, the length and radius of two guiding electrodes are $L=445.0$ mm and $r_0=1.0$ mm, respectively, and the half distance between the centers of two electrodes is $a=2.0$ mm, and the distance between the grounded metal plate and the center of the guiding electrodes is $b=10.0$ mm, and the two electrodes are charged by a high voltage source. We use the finite element software to calculate the spatial distribution of the electrostatic field produced by our charged-rod layout and find that there is a hollow quadrupolelike electrostatic field distribution (i.e., a hollow electrostatic tube) with a central minimum between two electrodes, as shown in Fig. 1(a), so our scheme can be used to realize the electrostatic guiding of cold polar molecules in the LFS states, and the resulting dipole force will push cold polar molecules to the minimum of the electric field. Because both the supersonic molecular beam and the ionized YAG laser beam are pulsed with a repetition frequency of 10 Hz, we employ a five-channel digital pulse generator to form a time-sequence controlling and synchronizing system so as to make sure that the YAG laser pulse shoots as soon as the guided molecules arrive at the ionizing region. In the experiment, the open width of the pulse valve is 400 μs, the mean velocity of the D_2O beam after the skimmer is about 550 m/s with a velocity spread (full width at half maximum) of about 28%, corresponding to a translational temperature of 16.3 K, and the corresponding transverse temperature is about 61.3 mK.[17]

III. THEORY AND MODELING

A. Theoretical calculation of absolute guiding efficiency

When the D_2O molecules are regarded as classical particles in the course of the guiding, the distributions of the position and velocity of the molecules before they enter the electrostatic tube are $f_p(x,y)$ and $f_v(v_x,v_y,v_z)$, respectively. We assume that the velocity distribution function $f_v(v_x,v_y,v_z)$ can be resolved into three components that are perpendicular to each other. So the distribution function can be written as

$$f(x,y;v_x,v_y,v_z)=f_p(x,y)f_v(v_x,v_y,v_z)=f_p(x,y)f_v(v_x)f_v(v_y)f_v(v_z), \tag{1}$$

and we have

$$f_v(v_x)=\sqrt{m/2\pi kT_t}\times\exp(-(mv_x^2/2kT_t)), \tag{2}$$

$$f_v(v_y)=\sqrt{m/2\pi kT_t}\times\exp(-(mv_y^2/2kT_t)), \tag{3}$$

$$f_v(v_z)=kv_z^2\exp(-(m(v_z-u)^2/2kT_l)\ , \tag{4}$$

where T_t and T_l are the transverse and translational (longitudinal) temperatures of the molecular beam, respectively, m the molecular mass, u the most probable velocity of molecular beam, and k the constant. The input flux can be expressed by

$$J_{\mathrm{in}}=\int_{p(x,y)}f_p(x,y)dxdy\int_{v_z>0}f(v_x)f(v_y)f(v_z)v_z dv_x dv_y dv_z=k\int_0^\infty v_z^3\exp(-m(v_z-u)^2/2kT_l)dv_z, \tag{5}$$

where $f_p(x,y)$ is the two-dimensional (2D) position distribution of the incident molecular beam at the entrance of the electrostatic tube.

The total energy of the molecules in the electrostatic field, i.e., kinetic energy plus Stark potential energy, is conservative. The motion of the guided molecules in the velocity region S must satisfy the energy conservation law as follows:

$$S(v_x,v_y):mv_x^2/2+mv_y^2/2<W_x+W_y. \tag{6}$$

That is to say, the cold molecules that can be bounded by the electrostatic potential must satisfy the above condition, W_x and W_y are the interaction Stark potentials of polar molecules with the electrostatic field in the x and y directions, respectively.

The output flux of the guiding molecular beam can be derived by

$$J_{\text{out}} = \int_{p(x,y)} f'_p(x,y)dxdy \int_{S(v_x,v_y),v_z>0} f(v_x)f(v_y)f(v_z)v_z dv_x dv_y dv_z$$
$$= k\int_0^\infty v_z^3 \exp(-m(v_z-u)^2/2kT_l)dv_z \int_{S(v_x,v_y)} f(v_x)f(v_y)dv_x dv_y, \quad (7)$$

where $f'_p(x,y)$ is the 2D position distribution of the output beam at the outlet of the electrostatic tube.

Then the absolute guiding efficiency can be defined as

$$\eta = J_{\text{out}}/J_{\text{in}}. \quad (8)$$

Substituting Eqs. (5) and (7) into Eq. (8), we can obtain the absolute guiding efficiency of the guided molecular beam.

B. Details of Monte Carlo simulations

D_2O is an asymmetric top molecule with rotational constants of $A=15.39\ \text{cm}^{-1}$, $B=7.26\ \text{cm}^{-1}$, and $C=4.85\ \text{cm}^{-1}$, and its electric dipole moment is 1.87 D.[18] The rotational energy levels of D_2O molecule are quite different from that of H_2O due to the difference of their rotational constants, and the energy differences between the D_2O molecular levels are smaller, so the D_2O levels are denser. In addition, D_2O molecule has a larger Stark shifts than H_2O one in the same electric field.

In the supersonic expansion, the molecular beam is rotationally and vibrationally cooled, and almost all molecules are populated in the vibrational and electronic ground states. Under the condition of thermal equilibrium, the relative population of the different rotational states is determined by the Boltzmann distribution and by their degeneracy. For the sake of simple and convenient, in our simulation, we assume that the reasonable rotational temperature of the supersonic molecular beam is equal to 20 K, which is higher than its translational temperature. In this case, more than 97% D_2O molecules in our guided molecular beam are populated in the LFS states of $J\leqslant 2$, in which the populations of the $|1,1,1\rangle$ and $|1,0,0\rangle$ states are about 37% and 22%, respectively.[19]

The Stark shift of each rotational state of D_2O molecule in the electrostatic field can be calculated by the Hamiltonian (including rotational Hamiltonian and Stark interaction Hamiltonian) as follows:[7,9]

$$H = H_{\text{rot}} + H_{\text{Stark}} = AJ_a^2 + BJ_b^2 + CJ_c^2 - \boldsymbol{\mu}\cdot E(\mathbf{r}), \quad (9)$$

where J_a, J_b, and J_c are the components of the angular momentum along the three principal axes of inertia, with corresponding rotational constants A, B, and C, and $-\boldsymbol{\mu}\cdot E(\mathbf{r})$ is the Stark interaction potential of the molecular dipole moment $\boldsymbol{\mu}$ with the electric field $E(\mathbf{r})$. Following Ref. 9, the eigenvalues $E_{J\tau M}$ and eigenfunctions $|J,\tau,M\rangle$ of the asymmetric rotor can be described as the superposition of symmetric-rotor eigenfunctions $|J,K,M\rangle$ and obtained by diagonalizing the Hamiltonian matrix in a truncated basis functions. For the symmetric rotor, K and M denote the projection of the total angular momentum J on the molecular symmetry axis (one of rotor body-fixed axis, in general, regarded as the axis of the highest symmetry) and on the z axis (i.e., the direction of the external E-field). For the asymmetric rotor, K is not a good quantum number, the pseudoquantum number τ ($\tau=K_- - K_+$) is introduced to express the wave functions $|J,\tau,M\rangle$ of the asymmetric rotor, and K_- and K_+ denote the prolate and the oblate top limits, respectively. A reasonable approximation for the Stark shift calculation of D_2O can be described by second-order perturbation. The Stark shifts can be obtained by numerically diagonalizing the Stark Hamiltonian ($J_{\max}=12$) for D_2O. From the above method, we calculate the Stark shift of D_2O molecule in our electrostatic field and find that the LFS states of D_2O have quadratic Stark shifts, that is, the Stark shift of each LFS state of D_2O in the electric field $E(r)$ can be fitted to a quadratic polynomial,

$$W(\mathbf{r}) = \alpha + \beta E(\mathbf{r}) + \gamma E(\mathbf{r})^2, \quad (10)$$

where α, β, and γ are the fit coefficients. The electric field E of an ideal hexapole is given by[20]

$$E(\mathbf{r}) = 3U_0\mathbf{r}^2/r_1^3, \quad (11)$$

where U_0 is the voltage applied to each set of hexapole rods, r_1 the inner radius of the hexapole, and r the radial spatial coordinate.

According to the Possion equation and method of images,[21] we can derive the following equations to calculate the electric field distribution in free space generated by our two-charged-wire system,

$$E_x(x,y) = C((x-a)/((x-a)^2+y^2) + (x+a)/((x+a)^2+y^2)$$
$$-(x-a)/((x-a)^2+(y-2b)^2)$$
$$-(x+a)/((x+a)^2+(y-2b)^2)$$
$$-(x-a)/((x-a)^2+(y+2b)^2)$$
$$-(x+a)/((x+a)^2+(y+2b)^2)), \quad (12)$$

$$E_y(x,y) = C(y/((x-a)^2+y^2) + y/((x+a)^2+y^2)$$
$$-(y-2b)/((x-a)^2+(y-2b)^2)$$
$$-(y-2b)/((x+a)^2+(y-2b)^2)$$
$$-(y+2b)/((x-a)^2+(y+2b)^2)$$
$$-(y+2b)/((x+a)^2+(y+2b)^2)), \quad (13)$$

where C is a constant. The above equations are derived by assuming that the charged wires and grounded plate are infinitely long in the z direction. Then the total electric field distribution is given by

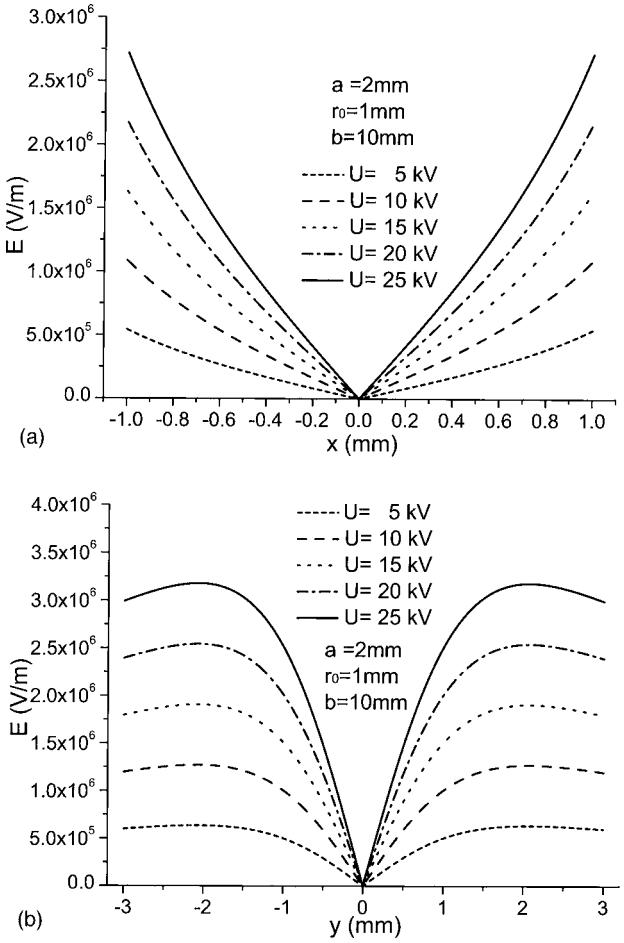

FIG. 2. The relationships between the guiding voltage U applied on the rods and the electric field distributions in (a) the x direction and (b) the y direction for $a=2.0$ mm, $b=10.0$ mm, and $r_0=1.0$ mm under the different guiding voltages.

$$|\mathbf{E}(x,y)| = \sqrt{E_x^2(x,y) + E_y^2(x,y)}. \tag{14}$$

The constant C can be calculated by solving the equation

$$\int_0^b |\mathbf{E}(x,y)|dy = U \tag{15}$$

when

$$x = \pm a,$$

where U is the guiding voltage added on the wires.

Also, we can use the finite element software to calculate the spatial distribution of the electrostatic field produced by our charged-wire layout and find that the calculated results from the above methods are identical except near the inlet and outlet of the charged electrodes.

We use a set of experimental parameters to calculate the spatial distributions of the electrostatic field in the x and y directions, and the results are shown in Fig. 2. It can be seen from Fig. 2 that the higher the guiding voltage U is, the larger the gradient of the electric field ($E(x)$ or $E(y)$) near the guiding center is, and the greater the maximum electric field $E(x)_{\max}$ or $E(y)_{\max}$ in the guiding region is, and then the deeper the 2D Stark potential well is, and the more the guided cold molecules is.

To obtain some parameters of the guided molecular beam and make the comparison with our experimental results, we study the dynamic process of the electrostatic guiding of cold D_2O molecules by using the classic Monte Carlo simulation[9] and Newton's motional equation.

Due to Stark effect, the D_2O molecules moving in the electrostatic field experience a dipole gradient force, which can be given by

$$\mathbf{F}(\mathbf{r}) = -\nabla W(\mathbf{r}) = m\ddot{r}, \tag{16}$$

where $W(\boldsymbol{r})$ is the Stark potential. From Eqs. (10) and (16), we performed Monte Carlo simulations for the guided D_2O molecular beam. In our simulation, the number of the simulated molecules is 10^4, and the considered Stark levels are all the LFS states of $J \leqslant 2$, and the transverse and longitudinal temperatures of our incident supersonic D_2O molecular beam are 61.3 mK and 16.3 K, respectively. We assume that the initial distribution of simulated molecular number at the incident plane satisfies a Gaussian one, and its transverse and longitudinal velocity distributions are given by Eqs. (2)–(4), and the simulated molecular trajectory is started from the nozzle, and the transverse size of the incident molecular beam is $d=0.5$ mm, which is equal to the diameter of the nozzle. The simulated molecules in each LFS state with the initial velocities and positions in the x, y, and z directions move starting from the inlet of the hexapole electrostatic lens and ended at the outlet of the electrostatic guiding tube, and then the velocities and positions of the guided molecules are recorded at the exit end of the guiding tube. The initial molecular number in each rotational state (including each Stark splitting state) is weighted by their populations, and on the output side, all the guided molecular number are summed for all weighted rotational states, which are the same as the initial rotational states.

IV. ANALYSIS AND RESULTS

Since our guiding scheme is a straight line guiding one, and the longitudinal most probable speed of the supersonic D_2O beam is very fast, the longitudinal motion of D_2O molecules in the supersonic beam will be nearly not disturbed during the molecular guiding process, while its transverse motion will be confined by the transverse Stark potential from the hollow electrostatic field, which will be determined by the applied guiding voltage on the two electrodes. The quadrupolelike electrostatic field forms a two-dimensional potential well, and the interaction potential of cold polar molecules with the electrostatic field depends on the internal states of the guided molecules. Some hot molecules, whose transverse kinetic energy exceeds the maximum transverse potential depth, cannot be guided in our hollow electrostatic pipe and pumped away by the molecular pump as the guiding voltage $V_{\text{guide}} \leqslant 25$ kV. However, many cold molecules with lower transverse kinetic energies can be efficiently guided in our hollow electrostatic pipe and exported from the sampling hole and reach our detecting region. In order to detect the guided D_2O molecules, we use the time-of-flight (TOF) mass spectroscopy to measure the guiding molecular signal. A Teflon sampling hole with a diameter of 2 mm,

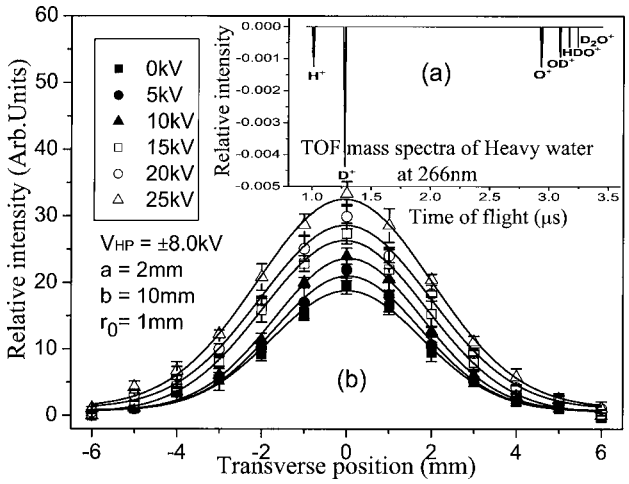

FIG. 3. (a) Time-of-flight mass spectra of pulsed D_2O molecule seeded in 2 atm argon ionized by pulsed of 266 nm laser with a pulse energy of 10.5 mJ. (b) The relative ion signal intensity of the guided D_2O molecules vs the transverse position for U=0, 5.0, 10.0, 15.0, 20.0, and 25.0 kV when a=2 mm, b=10 mm, r_0=1 mm, and V_{HP}= ± 8.0 kV. The symbols (black or hollow squares, circles, and triangles) with the corresponding error bars represent the experimental data points under the different guiding voltages, and the solid lines are the theoretically fitted curves by Gaussian profile.

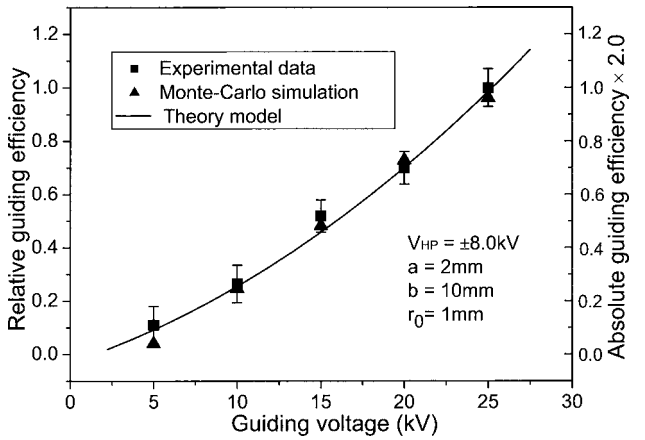

FIG. 4. The dependence of the relative guiding efficiency of cold molecules on the guiding voltage for a=2 mm, b=10 mm, r_0=1 mm, and V_{HP} = ± 8.0 kV. The black squares are the experimental data points including the corresponding error bars, the black triangles represent the Monte Carlo simulated results, while the solid line is the calculated results based on our theory model.

placed at the outlet of our guiding electrodes, is used to sample the guided D_2O molecular beam and filter the most of stray molecular scattering background. A pulsed 266 nm YAG laser (10 Hz) is used to ionize the guided D_2O molecules, and the ionized molecular ions are measured by the MCP detector after 250 mm field-free flight, and the total voltage on the extraction grid plate is 2200 V, and the signals are averaged over 300 shots. From the above analysis, we know that the guiding effect of cold molecules mostly happens in the transverse direction. In our experiment, consequently, we just measured the transverse distribution of the guided D_2O molecular beam under the different guiding voltages. Since the detected ion signal is proportional to the number N of the guided molecules, the ion signals will show the relative guiding efficiency of our guiding system. There are six ion signal peaks in the TOF mass spectrum of D_2O molecules at 266 nm (as shown in the inset of Fig. 3); they are mainly D^+, O^+, OD^+, and D_2O^+, respectively, including H^+, HDO^+ caused by the impurity embedded in heavy water. The sum of the curve-integrated areas under these ion peaks represents the relative number N of the guided D_2O molecules.

The measured transverse distribution of the guided D_2O molecular beam and its dependence on the guiding voltage are shown in Fig. 3(b), respectively. We can find from Fig. 3(b) that the higher the guiding voltage is, the higher the relative ion signal intensity is, and all transverse distributions of the guided D_2O beam are Gaussian ones, which can be fitted by the function $f(r)=k\exp(-r^2/r_0^2)$ [as shown in Eqs. (2) and (3)], where k and r_0 are the constant and the position spread of the guided molecule beam, respectively. It is obvious that the integrated area of each transverse distribution is proportional to the flux J_{out} (or the number N) of the guided D_2O molecules, and this flux depends on the transverse Stark potential for D_2O molecules, which is determined by the applied guiding voltage on the two electrodes.

It is clear that the ion signal without a guiding voltage is a straight transmission signal, not a guiding one, so a real and net guiding single must be a difference between the total ion signal with a guiding voltage of $V_{guide} \neq 0$ kV and the ion one without a guiding voltage (i.e., as $V_{guide}=0$ kV). The experimental dependence of the relative guiding efficiency on the guiding voltage is shown in Fig. 4. Each datum (the black squares) in Fig. 4 represents a difference between each integrated area under each transverse profile with a guiding voltage of $V_{guide} \neq 0$ kV, as shown in Fig. 3 and an integrated area without a guiding voltage of $V_{guide}=0$ kV, and the relative guiding efficiency is defined as the ratio of each subtracted integrated area at each guiding voltage to the corresponding value with a guiding voltage of 25.0 kV. We study the dependence of the relative guiding efficiency of cold molecules on the guiding voltage, and the experimental results (the black squares), the theoretically calculated results (the solid curve), and Monte Carlo simulated results (the black triangles) are shown in Fig. 4, respectively. In Fig. 4, the integrated area under each transverse profile as shown in Fig. 3(b) is proportional to the number N of the guiding molecules, and the solid curve is calculated by Eq. (8). It is clear from Fig. 4 that the higher the guiding voltage is, the higher the relative guiding efficiency is, and the experimental results are in good agreement with the both calculated and simulated ones. In our experiment, we can only measure the relative guiding efficiency, but by comparing it with the absolute one by our theoretical calculation and simulating, we can estimate the absolute guiding efficiency of our quadrupolelike guiding scheme. We can see from Fig. 4 that the maximum absolute guiding efficiency of our guiding scheme can reach ~50% as the guiding voltage is equal to 25 kV.

Also, we observed the transverse velocity distribution of the guided D_2O molecular beam and studied the dependence of the transverse temperature on the guiding voltage, and the experimental results are shown in Fig. 5. We can find from Fig. 5 that the transverse temperature of the guided molecular beam is increased with the increase of the guiding volt-

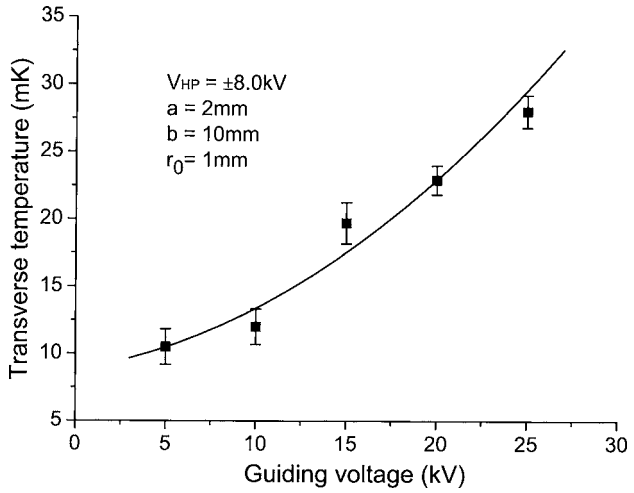

FIG. 5. The dependence of the transverse temperature of the guided molecular beam on the guiding voltage for $a=2$ mm, $b=10$ mm, $r_0=1$ mm, and $V_{HP}=\pm 8.0$ kV, the black squares represent the experimental data, including the corresponding error bars, and the solid line is the theoretically fitted curve.

age, and the transverse temperature is increased from about 10 to 28 mK when the guiding voltage is increased from 5 to 25 kV. This because the higher the guiding voltage is, the deeper the transverse well depth of our guiding system is, and then the higher the guiding efficiency is, and the higher the transverse temperature of the guided molecular beam is.

V. CONCLUSIONS

We have demonstrated the quadrupolelike electrostatic guiding of cold D_2O molecules by using a hollow electrostatic field and measured the transverse distributions of the guided molecular beam under the different guiding voltages, and studied the dependence of the relative guiding efficiency on the guiding voltage. Also, we have observed the dependence of the transverse temperature of the guided molecular beam on the guiding voltage. Our study shows that the relative guiding efficiency of the guided molecular beam and its transverse temperature are increased with increasing the guiding voltage V_{guide} and our experimental results are in good agreement with ones of the calculations and Monte Carlo simulations, and the maximum guiding efficiency can reach ~50% by using our guiding scheme as the guiding voltage is 25 kV.

In comparison with the standard quadrupole electrostatic guiding scheme,[9–11] our two-wire guiding one has two main advantages. (1) Our guiding efficiency is higher, this is because the voltages (or potentials) on our two-charged wires are identical, and the distance b between the charged wires and the grounded metal plates is large enough, we do not need to consider the discharge effect between the two wires, or between the charged wire and the grounded plate. So we can choose the space $2a$ between the two wires as small as possible, and the guiding voltage on the two wires as high as possible, and then we can obtain a deeper well depth and a higher guiding efficiency. (2) Our guiding scheme is simpler, and cold molecular beam is guided between two charged wires, so it can be used to form various molecule-optical elements, such as Y-shaped molecular-beam splitter (similar to one[22]), molecule interferometer, and so on, also to guide other species of cold polar molecules, even to generate a continuous-wave cold molecular beam by using an electrostatic bent guide.[9] Therefore, our guiding scheme has some new and important applications in molecule optics, particularly in integrated molecule optics.

ACKNOWLEDGMENTS

We would like to thank Dr. Xiaohua Yang, Dr. Jinming Liu, Min Yun, Qi Zhou, Guangbing Fu, and Yang Liu for their help in the experiment. This work is supported by the National Nature Science Foundation of China under Grant Nos. 10374029, 10434060, and 10674047, the National Key Basic Research and Development Program of China under Grant No. 2006CB921604, the Science and Technology Commission of Shanghai Municipality under Grant No. 04DZ14009, the Basic Key Program of Shanghai Municipality under Grant No.07jc14017, the Shanghai Priority Academic Discipline, and the 211 Foundation of the Educational Ministry of China.

[1] J. J. Hudson, B. E. Sauer, M. R. Tarbutt, and E. A. Hinds, Phys. Rev. Lett. **89**, 023003 (2002).
[2] J. J. Gilijamse, S. Hoekstra, S. Y. T. Meerakker, G. C. Groenenboom, and G. Meijer, Science **313**, 1617 (2006).
[3] E. R. Hudson, C. Ticknor, B. C. Sawyer, C. A. Taatjes, H. J. Lewandowski, J. R. Bochinski, J. L. Bohn, and J. Ye, Phys. Rev. A **73**, 063404 (2006).
[4] D. DeMille, Phys. Rev. Lett. **88**, 067901 (2002).
[5] A. André, D. DeMille, J. M. Doyle, M. D. Lukin, S. E. Maxwell, P. Rabl, R. J. Schoelkopf, and P. Zoller, Nat. Phys. **2**, 636 (2006).
[6] H. L. Bethlem, G. Berden, and G. Meijie, Phys. Rev. Lett. **83**, 1558 (1999).
[7] A. Schwettmann, J. Franklin, K. R. Overstreet, and J. P. Shafferar, J. Chem. Phys. **123**, 194305 (2005).
[8] H. L. Bethlem, G. Berden, F. M. H. Crompvoets, R. T. Jongma, A. J. A. Roij, and G. Meijer, Nature (London) **406**, 491 (2000).
[9] T. D. Hain, R. M. Moision, and T. J. Curtiss, J. Chem. Phys. **111**, 6797 (1999).
[10] D. Matsiev, J. Chen, M. Murphy, and A. M. Wodtke, J. Chem. Phys. **118**, 9477 (2003).
[11] H. J. Loesch and B. Scheel, Phys. Rev. Lett. **85**, 2709 (2000).
[12] S. A. Rangwala, T. Junglen, T. Rieger, P. W. H. Pinkse, and G. Rempe, Phys. Rev. A **67**, 043406 (2003).
[13] T. Junglen, T. Rieger, S. A. Rangwala, P. W. H. Pinkse, and G. Rempe, Phys. Rev. Lett. **92**, 223001 (2004).
[14] T. Rieger, T. Junglen, S. A. Rangwala, G. Rempe, and P. W. H. Pinkse, Phys. Rev. A **73**, 061402 (2006).
[15] Y. Xia, L. Deng, and J. Yin, Appl. Phys. B: Lasers Opt. **81**, 459 (2005).
[16] L. Z. Deng, Y. Xia, and J. P. Yin, Chin. Phys. Lett. **22**, 1887 (2005).
[17] The longitudinal velocity distribution of a supersonic beam in terms of molecular number density can be written as a shifted Maxwellian distribution function: $f(v)=kv_z^2\exp(-(v_z-u)^2/v_a^2)$, where u is the most probable velocity, v_a the width of the distribution, and k the constant, and the translational temperature of the molecular beam is given by the following equation; $T=(\frac{1}{2}mv_a^2)/k_B$. Similarly, the transverse temperature of the molecular beam can be given by $T=(\frac{1}{2}mv_b^2)/k_B$, v_b is the full width at half maximum of the transverse velocity spread in the center of the molecular beam.
[18] C. H. Townes and A. L. Schawlow, *Microwave Spectroscopy* (Dover, New York, 1975), p. 639.
[19] W. Gordy and R. L. Cook, *Microwave Molecular Spectra* (Wiley, New York, 1984), p. 54.
[20] R. B. Bernstein, *Chemical Dynamics via Molecular Beam and Laser Techniques* (Oxford University Press, New York, 1982), Chap. 3, p. 25.
[21] W. H. Hayt, Jr. and J. A. Buck, *Engineering Electromagnetics*, 6th ed. (McGraw-Hill, New York, 2001), Chap. 5.5, p. 134.
[22] L. Z. Deng and J. P. Yin, Opt. Lett. **32**, 1695 (2007).